

## Kinetics of the photoinduced dissociative reduction of the model alkyl peroxides di-*tert*-butyl peroxide and ascaridole

David C. Magri<sup>1\*</sup> and Mark. S. Workentin<sup>2</sup>

<sup>1</sup>Department of Chemistry, University of Malta, Msida, Malta, MSD 2080.

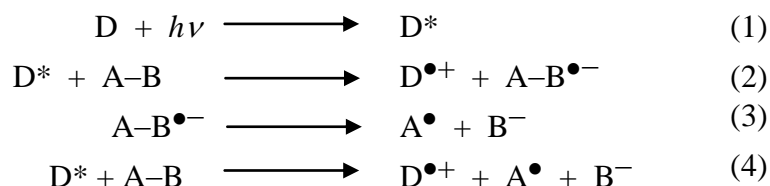
<sup>2</sup>Department of Chemistry, The University of Western Ontario, London, Ontario, Canada N6A 5B7.

**Abstract:** Rate constants for the reaction between excited singlet state aromatic donors and the dialkyl peroxide, di-*tert*-butyl peroxide (DTBP), and the bicyclic endoperoxide, ascaridole (ASC), were measured in acetonitrile using fluorescence quenching techniques. The rate constants, measured with 18 different aromatic donors by Stern-Volmer quenching, range from  $9.2 \times 10^9$  to  $4.4 \times 10^6 \text{ M}^{-1} \text{ s}^{-1}$ . Using accurately measured standard reduction potentials for the peroxides, the driving force for photoinduced electron transfer is predicted to be thermodynamically feasible over the entire range of excited donors ranging from  $-49$  to  $-10 \text{ kcal mol}^{-1}$  for ASC and  $-38$  to  $-2 \text{ kcal mol}^{-1}$  for DTBP. However, when the photoinduced kinetics are combined with previously measured electron transfer kinetics by homogeneous redox catalysis with ground state radical-anion donors, a smooth parabolic correlation for a dissociative electron transfer mechanism is not observed. Rather, a discontinuity is observed between the photochemical and electrochemical data sets with the rate constants with singlet excited states donors being over two orders of magnitude larger than the ground state kinetics at the same driving force. The discrepancy is examined considering the importance of attractive interaction between fragments in the dissociative photoinduced electron transfer reactions.

**Keywords:** photoinduced dissociative electron transfer, fluorescence, endoperoxide, Stern-Volmer, kinetics.

### Introduction

Photoinduced electron transfer (PET) reactions are often accompanied by cleavage of a frangible covalent bond<sup>1-4</sup>. Savéant developed a model, dissociative electron transfer (DET) theory, which takes into account ET reactions accompanied by bond breakage under electrochemical<sup>5,6</sup> and photochemical<sup>7</sup> conditions. In photoinduced DET reactions, the electron source is a photochemically excited state donor (eq 1). Transfer of an electron from a sensitizer ( $D^*$ ) to a substrate ( $A-B$ ) can involve either two successive steps (eq 2 and eq 3), or a single step (eq 4), depending on the existence of the radical-anion intermediate ( $A-B^{\bullet-}$ ) as shown in Scheme 1. ET involving two successive steps is commonly referred to as a stepwise dissociative mechanism, while ET involving only one step without a radical-anion intermediate as a concerted dissociative mechanism.

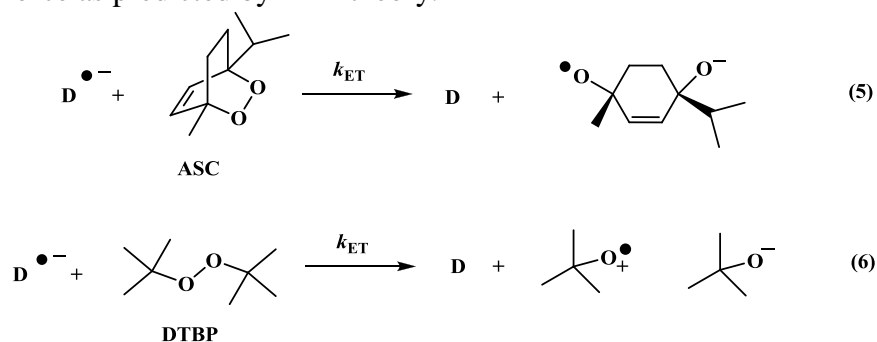


**Scheme 1:** Stepwise (eqs 1-3) versus concerted dissociative (eqs 1 and 4) PET.

\*Corresponding author:

E-mail address: [david.magri@um.edu.mt](mailto:david.magri@um.edu.mt)

The electrochemical reduction of dialkyl peroxides<sup>8,9</sup>, bicyclic endoperoxides<sup>10,11</sup> and perbenzoates<sup>12,13</sup> occurs by a dissociative ET mechanism resulting in cleavage of the O-O bond<sup>14</sup>. A few examples of stepwise dissociative ET mechanisms involving peroxide bonds are known,<sup>11a,11d,13</sup> although the vast majority of studies, including those of di-*tert*-butyl peroxide (DTBP)<sup>8</sup> and ascaridole (ASC)<sup>10</sup> are concerted. Reduction of ASC results in the initial formation of an intermediate with a spatially separated alkoxy radical and an alkoxide, termed a distonic radical-anion (eq 5), whereas ET transfer to DTBP results in the formation of an alkoxy radical and an alkoxide intermediates (eq 6). The resulting products after ET and protonation of the intermediates are the quantitative formation of *cis*-diol and *tert*-butyl alcohol, respectively. In both studies, ET rate constants were measured in *N,N*-dimethylformamide and acetonitrile using homogeneous radical-anion donors ( $D^{\bullet-}$ ) by homogeneous redox catalysis (Scheme 2)<sup>8,10</sup>. Accurate knowledge of  $E^{\circ}_{AB/A^{\bullet-}+B^-}$  allowed for the analysis of the homogeneous kinetics of ASC and DTBP as a function of driving force for ET,  $\Delta G_{ET}$ . Among many findings, the  $Z$  was determined to be two orders of magnitude lower than the commonly accepted adiabatic value of  $3 \times 10^{11} \text{ M}^{-1} \text{ s}^{-1}$ , providing the first examples of non-adiabatic dissociative ET<sup>8-10</sup>. Furthermore, these model systems because of their much weaker O-O bond, illustrated quite convincingly the parabolic dependence of the ET kinetics with driving force as predicted by DET theory.<sup>5</sup>



**Scheme 2** The initial reduction of ASC and DTBP with electrochemically-generated radical-anion donors.

Previous studies of ASC and DTBP from excited singlet and triplet donors concluded that the photoinduced reactions occur by an energy transfer mechanism<sup>15</sup>. An ET mechanism was ruled out because the feasibility for ET, calculated using the directly observed irreversible peak potentials from cyclic voltammetry, predicted an unfavourable driving force. However, we have shown that the irreversibly observed peak potentials previous used were in error by up to 1 V or 23 kcal mol<sup>-1</sup> due to the large overpotential from breaking of the O-O bond<sup>8-10</sup>. With knowledge of accurate standard reduction potentials for DTBP and ASC, PET is predicted to be readily thermodynamically feasible from singlet excited state donors. In our studies on the antimalarial endoperoxide, artemisinin, a concerted DET mechanism was suggested under both heterogeneous electrochemical<sup>16</sup> and photochemical conditions.<sup>17</sup>

Therefore, it was of interest to extend the kinetic and thermodynamic range of the existing homogeneous data to larger driving forces. Only in a few cases has an extensive series of kinetic data been measured electrochemically and extended to larger driving forces using a complimentary technique<sup>18</sup>. The ET reduction of *tert*-butyl bromide with aromatic radical-anion donors by homogeneous redox catalysis for the smaller rate constants, and pulse radiolysis for the larger rate constants, is the most comprehensive<sup>19</sup>.

The kinetic data measured by the two independent techniques, based on ET from aromatic radical anions, were found

to be compatible, and exhibited a continuous trend. However, it was difficult to decipher between a linear, or a parabolic correlation, the latter predicted by DET theory.

As supported by previous peroxide studies<sup>8-10</sup>, the lack of curvature observed with the *tert*-butyl bromide data is from the larger intrinsic barrier associated with concerted cleavage of the C-Br bond.

The objective of this study was to extend the previously measured kinetic and thermodynamic data for ASC and DTBP measured using electrochemically generated radical-anions to larger driving forces. This was carried out by measuring rate constants between a series of singlet excited state aromatic donors and the model peroxides DTBP and ASC in acetonitrile using fluorescence quenching techniques. With knowledge of the accurate standard reduction potentials, it was hypothesized that the kinetic data would extend the existing parabolic trend (as observed with *tert*-butyl bromide) for a concerted dissociative PET mechanism as observed with electrochemical methods. Rather we observe a discontinuity between the photochemical excited state and the ground state electrochemical kinetics as a function of the driving force for ET. The results highlight the importance of electrostatic interactions between fragments in photoinduced DET reactions.

## Results and Discussion

### Results

Bimolecular rate constants were measured in nitrogen-purged solutions of acetonitrile using a series of singlet excited state donors and steady-state fluorescence quenching techniques. The Stern-Volmer equation (eq 7) relates the quantum yield of the sensitizer fluorescence,  $\Phi_0^f$ , relative to the quantum yield in the presence of quencher,  $\Phi^f$ , as a function of quencher concentration, [Q], where  $k_{ET}$  is the rate constant of quenching, and  $\tau$  the lifetime of the sensitizer excited state. In practice, the fluorescence intensities rather than the quantum yields are used because of the ease of obtaining the measurements directly from emission spectra.

$$\frac{\Phi_0^f}{\Phi^f} = 1 + k_{ET}\tau[Q] \quad (7)$$

A series of 18 aromatic and amine sensitizers with varying oxidation potentials,  $E_{ox}$ , and singlet energies,  $E_S$ , were selected as quenchers. Table 1 lists the sensitizers and their photophysical properties. Fig. 1 illustrates the effect on the emission intensity of (a) *N,N,N',N'*-tetramethylbenzidine and (b) chrysene as the concentration of ASC is incrementally increased. For all sensitizers, the addition of ASC or DTBP results in a decrease in the fluorescence intensity and the absence of new emission bands. The fluorescence intensity ratio  $I_0^f/I^f$  was measured from an emission peak maximum (or peak area) at various concentrations and plotted versus [Q] according to eq 7. The Stern-Volmer plots were linear in all cases as illustrated in Fig. 2. with the coefficient of determination  $R^2 > 0.998$ . The fluorescence quenching rate constants were determined from the slopes of the linear fit, equal to  $k_{ET}\tau$ , and from published or measured fluorescence lifetimes,  $\tau$ .

**Table 1:** Photophysical data and oxidation potentials of the fluorescent sensitizers.

Donor	$E_{D^{•+}/D}$ V vs SCE	$E_S^a$ /kcal mol <sup>-1</sup>	$E_{D^{•+}/D^*b}$ /kcal mol <sup>-1</sup>	$\tau$ /10 <sup>-9</sup> s
<i>N,N,N',N'</i> -Tetramethylphenylenediamine	0.16 <sup>c</sup>	77.6	-73.7	7.1 <sup>d</sup>
<i>N,N,N',N'</i> -Tetramethylbenzidine	0.43 <sup>c</sup>	83.0	-73.1	10.0 <sup>e</sup>
<i>N,N</i> -Dimethylaniline	0.79 <sup>c</sup>	88.4	-70.1	2.8 <sup>d</sup>
<i>N,N</i> -Diethylaniline	0.76 <sup>c</sup>	87.6	-70.1	2.8 <sup>f</sup>
Acenaphthene	1.21 <sup>g</sup>	89.8	-61.9	39.6 <sup>h</sup>
Naphthalene	1.54 <sup>g</sup>	92.4	-56.9	105 <sup>i</sup>
9,10-Dimethylantracene	0.87 <sup>l</sup>	71.5	-51.4	11 <sup>i</sup>
Anthracene	1.09 <sup>g</sup>	76.2	-51.1	5.8 <sup>j</sup>
Pyrene	1.16 <sup>g</sup>	77.0	-50.3	323 <sup>h</sup>
Chrysene	1.35 <sup>g</sup>	79.6	-48.5	42.6 <sup>d</sup>
Benzo( <i>ghi</i> )perylene	1.01 <sup>g</sup>	71.4	-48.1	119 <sup>h</sup>
Phenanthrene	1.50 <sup>g</sup>	82.7	-47.2	57.5 <sup>k</sup>
Perylene	0.85 <sup>g</sup>	65.8	-46.2	6.0 <sup>j</sup>
9-Phenylanthracene	1.30 <sup>l</sup>	74.0	-44.0	6.8 <sup>i</sup>
Tetracene	0.77 <sup>l</sup>	60.9	-43.1	5.6 <sup>i</sup>
9,10-Diphenylanthracene	1.27 <sup>l</sup>	71.9	-42.6	8.2 <sup>i</sup>
Fluoranthene	1.45 <sup>g</sup>	72.9	-39.5	46.4 <sup>h</sup>
Coronene	1.23 <sup>g</sup>	66.1	-37.7	299 <sup>h</sup>

<sup>a</sup>Measured in acetonitrile. <sup>b</sup>Calculated from  $E_{D^{•+}/D^*} = 23.06(E_{D^{•+}/D} - E_S)$  <sup>c</sup>P. Iwa, U. E. Steiner, E. Vogelmann, H. E. A. Kramer, *J. Phys. Chem.* 1982, **86**, 1277. <sup>d</sup>I. B. Berlman, *Handbook of Fluorescence Spectra of Aromatic Molecules*; Second ed.; Academic Press, New York, 1971. <sup>e</sup>S. Hashimoto, J. K. Thomas, *J. Phys. Chem.* 1984, **88**, 4044. <sup>f</sup>A. E. W. Knight, B. K. Selinger, *Chem. Phys. Lett.* 1971, **10**, 43. <sup>g</sup>E. S. Pysh, N. C. Yang, *J. Am. Chem. Soc.* 1963, **85**, 2124. <sup>h</sup>Measured. <sup>i</sup>S. L. Murov, I. Carmichael, G. L. Hug, *Handbook of Photochemistry*, 2nd. ed. Marcel Dekker, New York, 1993. <sup>j</sup>W. R. Ware, *J. Phys. Chem.* 1962, **66**, 455. <sup>k</sup>W. L. Wallace, R. P. Van Duyne, F. D. Lewis, *J. Am. Chem. Soc.* 1976, **98**, 5319. <sup>l</sup>M. S. Workentin, V. D. Parker, T. L. Morkin, D. D. M. Wayner, *J. Phys. Chem. A* 1998, **102**, 6503.

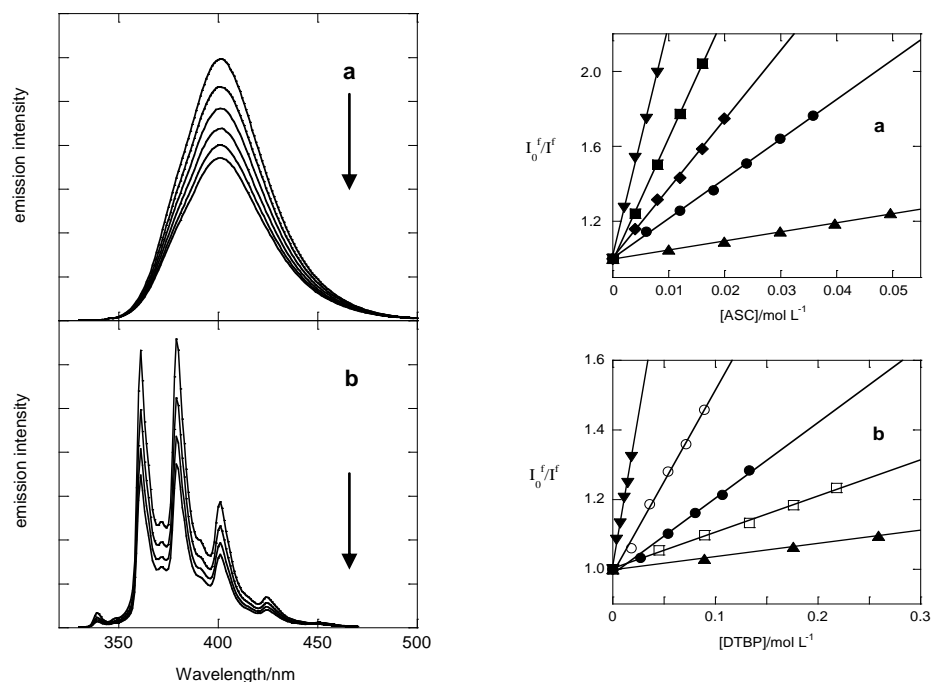


**Fig. 1 (left side)** Fluorescence quenching spectra of: (a) *N,N,N',N'*-tetramethylbenzidine in the presence of 0, 1.2, 2.4, 3.6, 4.8 and 7.2 mM ASC; (b) chrysene in the presence of 0, 12.0, 23.9 and 35.8 mM of ASC. As indicated with an arrow, the emission intensity decreases with increasing concentration of ASC. **Fig. 2 (right side)** Representative Stern-Volmer plots for (a) ASC and (b) DTBP quenching the fluorescence of various donors: ( $\blacktriangledown$ ) naphthalene, ( $\blacksquare$ ) acenaphthene, ( $\blacklozenge$ ) *N,N,N',N'*-tetramethyl-1,4-phenylenediamine, ( $\bullet$ ) chrysene, ( $\blacktriangle$ ) anthracene, ( $\circ$ ) phenanthrene, and ( $\square$ ) coronene.

**Table 2:** Bimolecular rate constants for excited state aromatic donors quenched by DTBP and ASC and the driving force for PET calculated for concerted and stepwise ET mechanisms.

Donors	$\Delta G_{\text{DTBP}}^{\text{a,b}}$	$\Delta G_{\text{DTBP}}^{\text{a,c}}$	$k_{\text{DTBP}}$	$\Delta G_{\text{ASC}}^{\text{a,d}}$	$\Delta G_{\text{ASC}}^{\text{a,e}}$	$k_{\text{ASC}}$
	(kcal/mol)	(kcal/mol)	(/10 <sup>7</sup> M <sup>-1</sup> s <sup>-1</sup> )	(kcal/mol)	(kcal/mol)	(/10 <sup>7</sup> M <sup>-1</sup> s <sup>-1</sup> )
	Concerted	Stepwise		Concerted	Stepwise	
<i>N,N,N',N'</i> - Tetramethylphenylenediamine	-38.0	-11.4	20	-48.6	-23.1	910
<i>N,N,N',N'</i> -Tetramethylbenzidine	-37.4	-10.8	82	-46.1	-20.6	510
<i>N,N</i> -Dimethylaniline	-34.5	-7.9	16	-45.5	-20.0	780
<i>N,N</i> -Diethylaniline	-34.4	-7.8	10	-42.5	-17.0	750
Acenaphthene	-26.3	0.4	36	-34.3	-8.9	240
Naphthalene	-21.2	5.4	18	-29.3	-3.8	140
9,10-Dimethylantracene	-15.8	10.8	2.4	-23.9	1.6	64
Anthracene	-15.4	11.2	6.6	-23.5	2.0	84
Pyrene	-14.6	12.0	1.6	-22.7	2.8	17
Chrysene	-12.8	13.8	4.2	-20.9	4.6	48
Benzo( <i>ghi</i> )perylene	-12.5	14.2	0.41	-20.5	4.9	6.5
Phenanthrene	-11.5	15.1	3.0	-19.6	5.9	59
Perylene	-10.6	16.1	4.3	-18.6	6.8	21
9-Phenylantracene	-8.4	18.2	7.6	-16.5	9.0	61
Tetracene	-7.5	19.1	2.0	-15.6	9.9	18
9,10-Diphenylantracene	-7.0	19.6	4.5	-15.0	10.4	38
Fluoranthene	-3.8	22.8	1.2	-11.9	13.6	7.8
Coronene	-2.1	24.5	0.44	-10.2	15.3	2.7

<sup>a</sup>Free energies calculated from the Weller equation:  $\Delta G_{\text{ET}} = 23.06 (E_{\text{D/D}^{\bullet+}}^{\circ} + E_{\text{D}_{\text{AB/A}^{\bullet+}\text{B}^-}^{\circ}} - q^2/\epsilon r) - E_{\text{s}}$  where  $q^2/\epsilon r = 0.1$  V;

<sup>b</sup> $E_{\text{AB/A}^{\bullet+}\text{B}^-}^{\circ}(\text{DTBP}) = -1.55$  V vs. SCE, <sup>c</sup> $E_{\text{AB/A}^{\bullet+}\text{B}^-}^{\circ}(\text{DTBP}) = -2.7$  V vs. SCE, <sup>d</sup> $E_{\text{AB/A}^{\bullet+}\text{B}^-}^{\circ}(\text{ASC}) = -1.2$  V vs. SCE, <sup>e</sup> $E_{\text{AB/A}^{\bullet+}\text{B}^-}^{\circ}(\text{ASC}) = -2.3$  V. The stepwise values for DTBP and ASC are approximated based on the observed trend within a series of perbenzoates. Ref 13.

The quenching rate constants measured for ASC and DTBP are listed in Table 2. A comparison of the rate constants with respect to a given sensitizer reveals the rate constants are greater for ASC than DTBP by one order of magnitude. This difference is attributed to steric hindrance from the *tert*-butyl groups shielding the O-O bond.<sup>8</sup> The rate constants span over 3 orders of magnitude ranging from  $5 \times 10^6$  to  $9 \times 10^9$  M<sup>-1</sup> s<sup>-1</sup>, the fastest observed rate constants for ASC approach the diffusion limit in acetonitrile of  $2 \times 10^{10}$  M<sup>-1</sup> s<sup>-1</sup> with a calculated driving force of  $-48$  kcal mol<sup>-1</sup>.

Many precautions were taken to ensure the reliability of the measured rate constants. UV-visible absorption spectra were recorded before and after each quenching experiment to safeguard against inner filter effects from absorption of light by the peroxides. UV-visible spectra were also independently taken of ASC and DTBP at the various concentrations used. At concentrations of 0.1 M, both peroxides exhibit a weak absorption tail in the UV spectrum up to 340 nm. Most sensitizers were excited at wavelengths greater than 340 nm, or required significantly less peroxide for efficient quenching. Hence, the likelihood of energy transfer is ruled out.<sup>7d,e</sup> Control quenching experiments were also performed to ensure against dilution effects using nitrogen-saturated acetonitrile as a quencher in volumes similar to the peroxides: in all cases no significant change were observed in the fluorescence intensity. Furthermore,

control experiments in the presence of 0.1 M TEAP, as in the electrochemical reactions, were found to be within experimental error. For example, the quenching rate constant for ASC in the presence of 0.1 M TEAP was  $4.0 \times 10^8 \text{ M}^{-1} \text{ s}^{-1}$  and in the absence of electrolyte the rate constant was  $4.8 \times 10^8 \text{ M}^{-1} \text{ s}^{-1}$ .

The rate constants are plotted versus the feasibility for ET,  $\Delta G_{\text{ET}}$ , in Fig. 3 and 4. In the electrochemical experiments with homogeneous radical-anion donors, the  $\Delta G_{\text{ET}}$  is calculated from the oxidation potential of the radical-anion donor,  $E^{\circ}_{\text{D}^{\bullet+}/\text{D}^{\bullet}}$ , and the dissociative reduction potential of the peroxide,  $E^{\circ}_{\text{AB}/\text{A}^{\bullet+}\text{B}^{\bullet-}}$ , in eV as given by eq 8

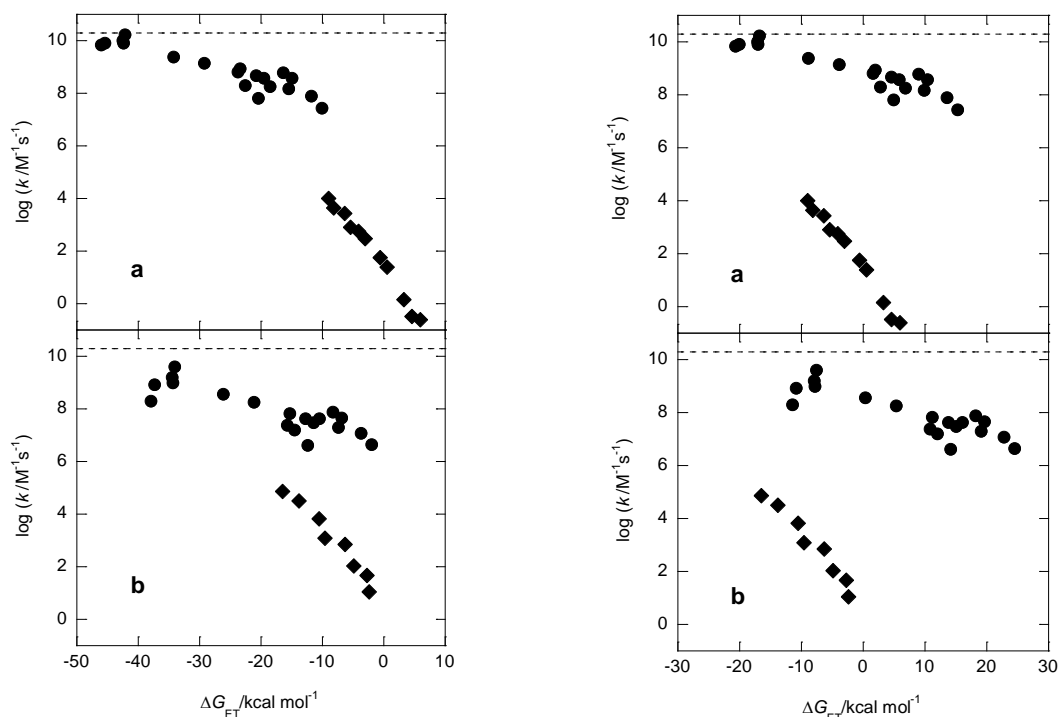


**Fig. 3 (left side)** The photochemical (●) and electrochemical (◆) ET rate constants of (a) ASC and (b) DTBP measured in acetonitrile. For both the electrochemical and photochemical rate constants,  $\Delta G_{\text{ET}}$  is calculated for a *concerted* dissociative mechanism. The dashed line is the diffusion limit in acetonitrile. **Fig. 4 (right side)** The photochemical (●) and electrochemical (◆) ET rate constants of (a) ASC and (b) DTBP measured in acetonitrile. For the electrochemical data,  $\Delta G_{\text{ET}}$  corresponds to a *concerted* mechanism and for the photochemical data,  $\Delta G_{\text{ET}}$  is calculated assuming a *stepwise* dissociative mechanism. The dashed line is the diffusion limit in acetonitrile.

$$\Delta G_{\text{ET}} = 23.06(E^{\circ}_{\text{D}^{\bullet+}/\text{D}^{\bullet}} + E^{\circ}_{\text{AB}/\text{A}^{\bullet+}\text{B}^{\bullet-}}) \quad (8)$$

In PET reactions, in addition to knowledge of the redox potentials, the  $\Delta G_{\text{ET}}$  is dependent on knowledge of the singlet energy of the donor,  $E_s$  in  $\text{kcal mol}^{-1}$  and the Coulombic term,  $q^2/\epsilon r$ , in eV. The latter takes into account the desolvation and attraction of solvent-separated oppositely charged species. In polar solvents, such as acetonitrile with a large dielectric constant ( $\epsilon = 36$ ), the Coulombic term provides a negligible contribution to the overall free

energy on the order of 0.1 eV. Hence, the driving force for PET is calculated using the Weller equation as given in eq 9

$$\Delta G_{\text{ET}} = 23.06 (E_{\text{D/D}\cdot^+}^{\circ} + E_{\text{D}_{\text{AB/A}\cdot^+ \text{B}^-}^{\circ}} - q^2/\epsilon r) - E_s \quad (9)$$

The quenching rate constants are reported in Table 2 as a function of the driving force for both a concerted and stepwise PET using eq. 9 and the singlet energies and donor oxidation potentials in Table 1. The standard reduction potentials for concerted DET were taken from previously published results<sup>8,10</sup> whereas the stepwise values were approximated from a thorough study on the ET reduction of perbenzoates<sup>13</sup>. In both cases, the rate constants increase as the reaction becomes more exothermic with those for ASC being consistently greater. This is partly due to a steric effect imposed by the bulky *tert*-butyl groups in DTBP compared to the unshielded O-O bond in ASC. A similar trend was observed on comparison of the heterogeneous ET rate constants for DTBP and di-*n*-butyl peroxide<sup>8</sup>.

The rate constants in Table 2 cover a thermodynamic range spanning over 35 kcal mol<sup>-1</sup>. ET is thermodynamically feasible for all sensitizers based on a concerted ET mechanism. In contrast, a stepwise ET is an uphill process for the majority of sensitizers except for those with rate constants approaching the diffusion limit. In Fig. 3 and 4 the kinetic data of the homogeneous radical-anion donors<sup>8,10</sup> are combined with the photoinduced data as a function of driving force for ET. Fig. 3 illustrates the photochemical rate constants predicted for a concerted dissociative ET and Fig. 4 for a stepwise dissociative ET, respectively. The combined collection of rate constants is the most comprehensive covering a free energy range in excess of 50 kcal mol<sup>-1</sup> and a kinetic range of over 11 orders of magnitude.

## Discussion

Both thermodynamic and kinetic factors govern the competition between a stepwise and concerted mechanistic pathway, as well as the magnitude of the observed ET rate constant,  $k_{\text{ET}}$ <sup>20</sup>. Differentiating between eq 2 and eq 4 is dependent on a number of parameters including the standard potential of the electron acceptor, intrinsic barrier  $\Delta G_0^\ddagger$ , temperature  $T$  and the pre-exponential factor  $Z$ <sup>13</sup>. The rate constant for ET for either eq 2 or eq 4 is described by eq 10

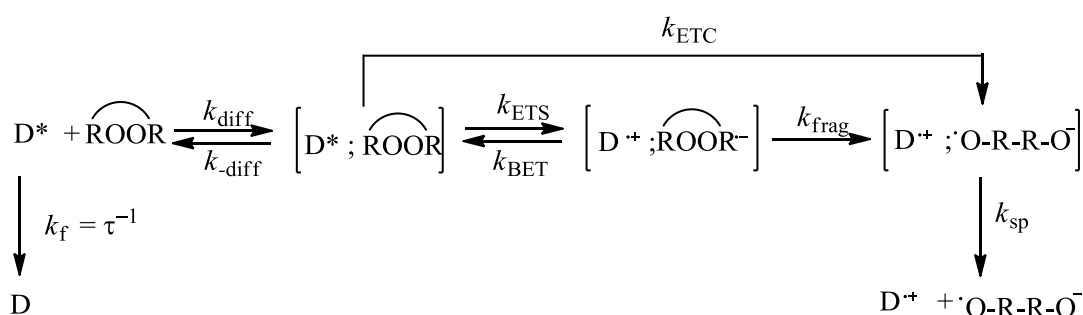
$$k_{\text{ET}} = Z \exp\left(-\frac{\Delta G^\ddagger}{RT}\right) \quad (10)$$

where  $\Delta G^\ddagger$  is the activation free energy. According to both non-dissociative and dissociative ET theories, the relationship between  $\Delta G^\ddagger$  and  $\Delta G_{\text{ET}}$ , the free energy for ET, is described by a quadratic activation-driving force relationship (eq 11)

$$\Delta G^\ddagger = \Delta G_0^\ddagger \left(1 + \frac{\Delta G_{\text{ET}}}{4\Delta G_0^\ddagger}\right)^2 \quad (11)$$

Concerted DET is thermodynamically favoured over the stepwise process when the standard potential for the concerted reduction,  $E_{\text{AB/A}\cdot^+ \text{B}^-}^{\circ}$ , is more positive than the standard potential for a stepwise reduction,  $E_{\text{AB/AB}\cdot^-}^{\circ}$ , and when the cleaving bond is weak, as commonly observed with peroxides. Scheme 3 highlights the two competing pathways.

In a stepwise mechanism (eq 2), the major contribution to the  $\Delta G_0^\ddagger$  is the solvent reorganization energy,  $\lambda$  according to  $\Delta G_0^\ddagger = \lambda/4$ . However, in a concerted mechanism (eq 4)  $\Delta G_0^\ddagger$  also has a significant contribution from  $D_R$ , the bond dissociation energy of the cleaving bond such that for a concerted dissociative ET  $\Delta G_0^\ddagger = (D_R + \lambda)/4$ . The pre-exponential factor for formation of the radical-anion intermediate (eq 2) and concerted DET (eq 4) typically describe an adiabatic process. However, with peroxides the concerted DET is non-adiabatic with the  $Z$  value at least 0.01 smaller than the adiabatic value<sup>8-10</sup>. With respect to  $\log k_{ET}$  versus  $\Delta G_{ET}$  plots, the  $Z$  and the standard potential directly affect the ordinate and abscissa, respectively. A smaller non-adiabatic  $Z$  results in a downward shift in the observed  $\log k_{ET}$  whereas a smaller (or more negative) standard potential results in a shift to less driving force. The intrinsic barrier describes the curvature of the parabola – as  $\Delta G_0^\ddagger$  increases, the parabola flattens in the downward direction.



**Scheme 3:** The mechanistic ET pathways for the photochemical reduction of endoperoxides (and peroxides) accounting for both concerted and stepwise dissociative PET. The rate constants are:  $k_f$  (fluorescence),  $k_{diff}$  (diffusion rate constant),  $k_{-diff}$  (back diffusion rate constant),  $k_{ETS}$  (stepwise ET),  $k_{BET}$  (back electron transfer),  $k_{ETC}$  (concerted ET),  $k_{frag}$  (fragmentation of the O-O bond) and  $k_{sp}$  (separation of ions).

In Fig. 3 (left side) the photochemically determined rate constants for both ASC and DTBP do not exactly follow the established trend of the electrochemical kinetics. The two kinetic sets for ASC display a discrepancy of 3 log units at  $\Delta G_{ET} = -10 \text{ kcal mol}^{-1}$ , where the electrochemical data ends and the photochemical data begins. With DTBP the discrepancy is most pronounced. The  $\Delta G^\ddagger$  for concerted dissociative ET to ASC and DTBP in the electrochemical experiments are 12 and 13  $\text{kcal mol}^{-1}$ , respectively, as previously reported<sup>7,8</sup>. This discrepancy of 3 log units between data sets corresponds to a  $\Delta\Delta G^\ddagger$  of 4  $\text{kcal mol}^{-1}$  between the photochemical and electrochemical data sets according to a concerted DET mechanism.

What is the source of this difference in the kinetic sets? PET reactions differ from electrochemical ET reactions with radical-anion donors in that the overall driving force is greater in the photochemical case. As the driving force for photoinduced reactions is larger, there is the possibility that the mechanism may switch to a stepwise mechanism as observed with 4-cyanobenzylmethylphenyl sulfonium on going from electrochemical to photochemical conditions<sup>7</sup>. In Fig. 4 (right side) the photochemical rate constants are plotted under the assumption of a stepwise ET mechanism (and the electrochemical data as a concerted ET mechanism). The PET rate constants are shifted to positive driving forces for the vast majority of donors. Although the intrinsic barrier is considerably smaller for a stepwise DET, based on thermodynamics, a stepwise DET reaction is not predicted to be feasible and a



change of mechanism unlikely. The same conclusion was reached with  $\text{CCl}_4$  and 4-cyanobenzyl chloride, which were shown to follow a concerted mechanism at low driving forces and a concerted mechanism with singlet excited state donors<sup>3b,7a</sup>. Another possibility could be an increase in the Z term – to the extreme that the rate of PET is faster by up to a factor of 100 at the largest driving forces such that PET to peroxides is an adiabatic reaction. However, we know of no precedence in this regard.

Another difference between PET and the ground state ET is with respect to the attractive interactions between intermediates. ET between radical-anion donors and a substrate, as in eqs 5 and 6, results in no net change in charge between reactants and products. However, ET between two neutral molecules results in the formation of a pair of oppositely charged species. Typically the formation of charged species is considered as a thermodynamic work term as in the Weller equation eq 9<sup>22</sup>. However, when there is an attractive interaction between a radical and ion upon bond cleavage, there can be a boost to the kinetics and/or decrease to the intrinsic barrier<sup>3b,7a,23</sup>. as the repulsive potential energy surface has a shallow but observable minimum as seen with  $\text{CCl}_4$ <sup>7c</sup>. The "sticky" DET model has also been applied to account for a discrepancy in the PET rate constant for the reaction between 2-ethyl-9,10-dimethoxyanthracene and 4-cyanobenzyl chloride<sup>3b</sup>.

To account for attractive interactions, the intrinsic barrier is calculated using equation 12 where  $D_R$  is the bond dissociation energy and  $D_P$  is the interaction energy between fragments. Table 3 compares the experimental rate constants for carbon tetrachloride, 4-cyanobenzyl chloride, ASC and DTBP together with theoretically predicted rate constants for the cases when attractive interactions are not considered (eq 11) and when there is an attractive interaction (eq 12)<sup>24</sup>. From our analysis we find a reasonable fit with  $\Delta G_0^\ddagger = 8.7 \text{ kcal mol}^{-1}$  and  $D_P = 0.06 \text{ V}$  for ASC, the latter falls in line with previously determined values for carbon tetrachloride and 4-cyanobenzyl chloride<sup>3b</sup>. In contrast, a good fit with DTBP results in unreasonable values of  $\Delta G_0^\ddagger = 4.4 \text{ kcal mol}^{-1}$  and  $D_P = 1.0 \text{ V}$ : the minimum possible value for  $\Delta G_0^\ddagger$  is expected to be  $9 \text{ kcal mol}^{-1}$  based solely on the  $D_R$ . Instead, in Table 3 theoretical values for  $k_{\text{ET}}$  are included for  $D_P = 0.1 \text{ V}$  for comparison. The results of the data analysis suggest that ASC fits the "sticky" DET model, and DTBP not so well.

$$\Delta G^\ddagger = \left( \frac{(\sqrt{D_R} - \sqrt{D_P})^2 + \lambda_o}{4} \right) \left( 1 + \frac{\Delta G^0 - D_P}{(\sqrt{D_R} - \sqrt{D_P})^2 + \lambda_o} \right)^2 \quad (12)$$

What could explain this finding? Perhaps with ASC the eclipsed lone pair orbitals on the oxygen atoms are readily accessible to the pi orbitals of the excited state aromatic hydrocarbons, which facilitates an attractive interaction at the transition state<sup>25</sup>. A cyclic configuration would also facilitate a weak interaction between the alkoxide radical and the alkoxide, which would be more stable than a conformation in which both oxygen atoms are apart. In contrast, DTBP has the lone pair orbitals on the oxygen atoms in a staggered conformation, and more importantly, the steric bulk of the *tert*-butyl groups prohibits any such interaction between the oxygen atoms and the excited state donors. The interpretation is that ascaridole may react via a PET mechanism and whereas DTBP may prefer some other competing mode of reactivity<sup>26</sup>.

**Table 3:** Comparison of thermodynamic and kinetic data for concerted dissociative ET reduction of carbon tetrachloride, 4-cyanobenzyl chloride, ASC and DTBP.

Compounds	$\Delta G_{ET}$	$\Delta G^{\ddagger c}$	Theoretical <sup>f</sup>	$\Delta G^{\ddagger g}$	Theoretical <sup>h</sup>	Experimental <sup>i</sup>
	kcal mol <sup>-1</sup>	kcal mol <sup>-1</sup>	$k_{et}/M^{-1} s^{-1}$	kcal mol <sup>-1</sup>	$k_{et}/M^{-1} s^{-1}$	$k_{et}/M^{-1} s^{-1}$
CCl <sub>4</sub> <sup>a</sup>	-26.8	9.1	$4 \times 10^4$	5.3	$3 \times 10^7$	$3.1 \times 10^{9a}$
	-19.0	11.9	$3 \times 10^2$	7.8	$4 \times 10^5$	$2 \times 10^{5j}$
4-CNbzCl <sup>b</sup>	-30.0	9.2	$3 \times 10^4$	5.5	$2 \times 10^7$	$2 \times 10^8$
ASC <sup>c</sup>	-29.3	1.9	$1 \times 10^8$	0.4	$2 \times 10^9$	$1.4 \times 10^9$
	-20.9	3.8	$4 \times 10^6$	1.7	$2 \times 10^8$	$4.8 \times 10^8$
	-10.2	7.4	$9 \times 10^3$	4.8	$8 \times 10^5$	$2.7 \times 10^7$
DTBP <sup>d</sup>	-26.3	3.4	$1 \times 10^7$	1.1	$4 \times 10^8$	$3.6 \times 10^8$
	-21.2	4.8	$9 \times 10^5$	2.2	$7 \times 10^7$	$1.8 \times 10^8$
	-10.6	8.5	$2 \times 10^3$	5.4	$3 \times 10^5$	$4.3 \times 10^7$

<sup>a</sup>Reference 7d with perylene: reported values  $\Delta G_{ET} = -1.161V$ ,  $\lambda_o = 15.8$  kcal mol<sup>-1</sup>,  $D_R = 2.84$  V,  $D_P = 0.062$  V,  $k_{et}$  calculated from Stern-Volmer constant  $18.4$  M<sup>-1</sup> and fluorescence lifetime of perylene; <sup>b</sup>Reference 3b with 2-ethyl-9,10-dimethoxyanthracene:  $\Delta G_{ET} = -1.30V$ ,  $\lambda_o = 16$  kcal mol<sup>-1</sup>,  $D_R = 2.82$  V,  $D_P = 0.058$  V; <sup>c</sup>Reference 10,  $D_R = 28$  kcal mol<sup>-1</sup>,  $\lambda_o = 20$  kcal mol<sup>-1</sup>,  $D_P = 0.06$  V; <sup>d</sup>Reference 8,  $D_R = 37$  kcal mol<sup>-1</sup>,  $\lambda_o = 16$  kcal mol<sup>-1</sup>,  $D_P = 0.1$  V; <sup>e</sup>equation 11; <sup>f</sup>equation 10 and 11 with  $Z(CCl_4) = 2.0 \times 10^{11}$ ,  $Z(4-CNbzCl) = 2.0 \times 10^{11}$ ,  $Z(ASC) = 8.0 \times 10^9$ ,  $Z(DTBP) = 3.0 \times 10^9$  at 298K; <sup>g</sup>equation 12; <sup>h</sup>equation 10 and 12 refer to f. <sup>i</sup>Photoinduced reactions except for j. <sup>j</sup>Homogeneous redox catalysis. Reference 27.

## Conclusion

Our initial hypothesis was that a concerted dissociative PET mechanism would follow the established quadratic trend of the electrochemical data. Rather, we observed a discontinuity between the electrochemical and photochemical rate constants despite using accurate standard reduction potentials for the peroxides and taking great care to ensure the quality of the kinetic data measured by Stern-Volmer quenching. Based on thermodynamic arguments, a stepwise DET is an uphill reaction and thus ruled out. Thus, at high driving forces, the dissociative reaction for ASC involves concerted electron transfer and bond breaking. The enhancement in the observed rate constants likely results from a small but significant attractive interaction between cage fragments in the PET reactions, as observed with carbon tetrachloride and 4-cyanobenzyl chloride, which contributes to lower the activation barrier, and hence increase the rate of the reaction as predicted by dissociative electron transfer theory accounting for attractive interactions between intermediates on ET<sup>3b</sup>.

## Acknowledgements

Financial support is acknowledged from the University of Malta, Natural Science and Engineering Research Council of Canada (NSERC), the Canadian Foundation for Innovation (CFI) and the University of Western Ontario.

## Experimental Section

Emission and excitation spectra were measured at room temperature using a Fluorolog-311 spectrofluorimeter interfaced to a personal computer running version 2.2 DataMax software for Windows. UV-visible absorption spectra were measured on a Varian Cary 100 double-beamed UV-visible spectrometer. Infra-red spectra were recorded neat on a Bomem MB 100 FT-IR spectrometer between NaCl plates. Nuclear magnetic resonance (NMR) spectra were recorded on a Varian XL 300 spectrometer using tetramethylsilane as the internal reference standard.  $^1\text{H}$  and  $^{13}\text{C}$  NMR spectra were recorded at 300.1 and 74.5 MHz, respectively. Mass spectrometry was performed on a MAT 8200 Finnigan high-resolution mass spectrometer by electron impact. Singlet lifetimes were measured using a PTI (Photon Technology International) luminescence system LS-100 spectrophotometer. Data acquisition was obtained using 2.03 LS-100 TC-SPC software on a Pentium 166 computer and data analysis was performed using TimeMaster version 1.2. Sample concentrations were prepared with the optical density between 0.2 and 0.3 at the excitation wavelength and purged for a minimum of 10 minutes.

The fluorescent donors were purchased from Aldrich. Scintillation or gold label grades with purity > 99% were used. Other solids of lesser purity were either sublimed or recrystallized prior to use. *N,N*-dimethylaniline and *N,N*-diethylaniline were fractional distilled under reduced pressure. Spectroscopic grade acetonitrile (BDH) was used as received. Di-*tert*-butyl peroxide was purchased from Aldrich and passed through activated alumina before use. Ascaridole was prepared by photo-oxygenation with  $\alpha$ -terpinene using a published procedure.<sup>28</sup> Ascaridole was purified by distillation at reduced pressure using a Kugelrohr apparatus.  $\alpha$ -Terpinene (85 %) was purchased from Fluka and used as received.

## Fluorescence Quenching Experiments

A stock solution of fluorescent donor was prepared with 10 mg samples in 100 mL solutions of acetonitrile for 15 minutes. Subsequent donor concentrations ranging from  $1.0 \times 10^{-4}$  to  $1.0 \times 10^{-6}$  M were prepared by dilution. The optical density of each solution was kept below 0.2 at the longest wavelength. Samples were contained in a  $0.7 \text{ mm}^2$  Suprasil quartz cell and sealed with a Teflon septum. Before the initial addition of peroxide, the donor solution was purged with nitrogen gas for at least 10 minutes to remove oxygen. Precautions were taken to prevent volume changes due to evaporation of solvent. ASC and DTBP were stocked in septum-sealed vials and purged with nitrogen before use. Rate constants were evaluated from Stern-Volmer plots with a minimum of five concentrations of peroxide from the average of three separate experiments. An absorption spectrum of the donor solution was taken before and after addition of peroxide during the quenching experiment to check that the peroxides were not absorbing light at the excitation wavelength.

## References

- 1 - E. R. Gaillard and D. G. Whitten, *Acc. Chem. Res.*, **1996**, 29, 292.
- 2 - (a) F. D. Saeva, *Top. Curr. Chem.* **1990**, 156, 61. (b) Saeva, F. D. in *Advances in Electron Transfer Chemistry*, Mariano, P. S. ed. JAI Press, New York, **1994**, vol 4, p. 1; (c) X. Wang, F. D. Saeva and J. A. Kampmeier, *J. Am. Chem. Soc.*, **1999**, 121, 4364; (d) J. A.

- Kampmeier, A. K. M. Hoque, F. D. Saeva, D. K. Wedegaertner, P. Thomsen, S. Ullah, J. Krake, and T. Lund, *J. Am. Chem. Soc.*, **2009**, *131*, 10015.
- 3 - (a) J. Bonin, C. Costentin, M. Mahet, J.-B. Mulon and Marc Robert, *Phys. Chem. Chem. Phys.*, **2009**, *11*, 10275; (b) L. Pause, M. Robert and J.-M. Savéant, *J. Am. Chem. Soc.*, **2000**, *122*, 9829; (c) S. M. Bonesi and R. Erra-Balsells, *J. Chem. Soc. Perkin Trans. 2*, **2000**, 1583; (d) L. Chen, M. S. Farahat, H. Gan, S. Farid and D. G. Whitten, *J. Am. Chem. Soc.*, **1995**, *117*, 6398; (e) L. Chen, M. S. Farahat, E. R. Gaillard, S. Farid and D. G. Whitten, *J. Photochem. Photobiol. A: Chem*, **1996**, *95*, 21.
- 4 - (a) J. Mohanty, H. Pal, S.K. Nayak, S. Chattopadhyay and A.V. Sapre, *Chem. Phys. Lett.* **2003**, *370*, 641; (b) J. Mohanty, H. Pal and A. V. Sapre, *J. Chem. Phys.*, **2002**, *116*, 8006; (c) J. Mohanty, H. Pal, S. K. Nayak, S. Chattopadhyay and A. V. Sapre, *J. Chem. Phys.*, **2002**, *117*, 10744; (d) S. Nath, A. K. Singh, D. K. Palit, A. V. Sapre and J. P. Mittal, *J. Phys. Chem. A*, **2001**, *105*, 7151; (e) S. Nath and A. V. Sapre, *Chem. Phys. Lett.* **2001**, *344*, 138.
- 5 - (a) J.-M. Savéant, in *Advances in Physical Organic Chemistry*, ed. T. T. Tidwell, Academic Press, New York, **2000**, vol. 35, p. 117; (b) J.-M. Savéant, in *Advances in Electron Transfer Chemistry*, ed. P. S. Mariano, JAI Press, Greenwich, CT, **1994**, vol 4, p. 53; (c) J.-M. Savéant, *Acc. Chem. Res.*, **1993**, *26*, 455; (d) C. Costentin, M. Robert and J.-M. Savéant, *Chem. Phys.*, **2006**, *324*, 40.
- 6 - (a) A. Houmam, *Chem. Rev.*, **2008**, *108*, 2180; (b) R. A. Rossi, A. B. Pierini and A. B. Penenory, *Chem. Rev.*, **2003**, *103*, 71.
- 7 - (a) L. Pause, M. Robert and J.-M. Savéant, *J. Am. Chem. Soc.*, **2001**, *123*, 4886; (b) M. Robert and J.-M. Savéant, *J. Am. Chem. Soc.*, **2000**, *122*, 514; (c) C. Costentin, M. Robert and J.-M. Savéant, *J. Phys. Chem. A*, **2000**, *104*, 7492; (d) L. Pause, M. Robert and J.-M. Savéant, *ChemPhysChem*, **2000**, *1*, 199.
- 8 - (a) R. L. Donkers, F. Maran, D. D. M. Wayner and M. S. Workentin, *J. Am. Chem. Soc.*, **1999**, *121*, 7239; (b) M. S. Workentin, F. Maran and D. D. M. Wayner, *J. Am. Chem. Soc.*, **1995**, *117*, 2120.
- 9 - (a) D. C. Magri and M. S. Workentin, *Org. Biomol. Chem.*, **2003**, *1*, 3418; (b) S. Antonello, M. Musumeci, D. D. M. Wayner and F. Maran, *J. Am. Chem. Soc.*, **1997**, *119*, 541.
- 10 - (a) R. L. Donkers and M. S. Workentin, *Chem.–Eur. J.*, **2001**, *7*, 4012; (b) M. S. Workentin and R. L. Donkers, *J. Am. Chem. Soc.*, **1998**, *120*, 2664.
- 11 - (a) D. L. B. Stringle, D. C. Magri and M. S. Workentin, *Chem –Eur. J.* **2010**, *16*, 178; (b) D. C. Magri and M. S. Workentin, *Chem. –Eur. J.* **2008**, *14*, 1698; (c) D. C. Magri and M. S. Workentin, *Org. Biomol. Chem.* **2008**, *18*, 3354; (d) F. Najjar, C. André-Barrès, C. Lacaze-Dufaure, D. C. Magri, M. S. Workentin and T. Tzèdakakis, *Chem.–Eur. J.* **2007**, *13*, 1174; (e) R. L. Donkers and M. S. Workentin, *J. Am. Chem. Soc.* **2004**, *126*, 1688.
- 12 - (a) F. Polo, S. Antonello, F. Formaggio, C. Toniolo and F. Maran, *J. Am. Chem. Soc.*, **2005**, *127*, 492; (b) S. Antonello, F. Formaggio, A. Moretto, C. Toniolo and F. Maran, *J. Am. Chem. Soc.*, **2003**, *125*, 2874; (c) S. Antonello, M. Crisma, F. Formaggio, A. Moretto, F. Taddei, C. Toniolo and F. Maran, *J. Am. Chem. Soc.*, **2002**, *124*, 11503; (d) S. Antonello, F. Formaggio, A. Moretto, C. Toniolo and F. Maran, *J. Am. Chem. Soc.* **2001**, *123*, 9577.
- 13 - (a) S. Antonello and F. Maran, *J. Am. Chem. Soc.*, **1999**, *121*, 9668; (b) S. Antonello and F. Maran, *J. Am. Chem. Soc.*, **1997**, *119*, 12595.

- 14 - (a) F. Maran, D. D. M. Wayner and M. S. Workentin, in *Advances in Physical Organic Chemistry*, ed. T. T. Tidwell and J. P. Richard, Academic Press, New York, **2001**, vol 36, 85. (b) F. Maran and M. S. Workentin, *Interface*, **2002**, 44.
- 15 - (a) M. V. Encinas, E. A. Lissi, *J. Photochem.* **1982**, *20*, 153; (b) P. S. Engel, T. L. Woods, M. A. Page, *J. Phys. Chem.* **1983**, *87*, 10; (c) J. C. Scaiano, G. G. Wubbels, *J. Am. Chem. Soc.* **1981**, *103*, 640.
- 16 - R. L. Donkers and M. S. Workentin, *J. Phys. Chem. B.* **1998**, *102*, 4061.
- 17 - D. C. Magri, R. L. Donkers and M. S. Workentin, *J. Photochem. Photobiol. A. Chem.*, **2001**, *138*, 29.
- 18 - (a) K. Daasbjerg, S. U. Pederson and H. Lund, *Acta Chem. Scand.*, **1991**, *45*, 424; (b) T. Lund and H. Lund, *Acta Chem. Scand. B*, **1986**, *40*, 470; (c) C. P. Andrieux, I. Gallardo, J.-M. Savéant and K.-B. Su, *J. Am. Chem. Soc.*, **1986**, *108*, 638; (d) S. Fukuzumi, S. Kuroda, and T. Tanaka, *J. Chem. Soc. Perkin Trans. 2*, **1986**, 25.
- 19 - (a) J. Grimshaw, J. R. Langan and G. A. Salmon, *J. Chem. Soc. Faraday. Trans.*, **1994**, *90*, 75; (b) J. Grimshaw, J. R. Langan and G. A. Salmon, *J. Chem. Soc. Chem. Comm.*, **1988**, 1115.
- 20 - N. Sutin, *Acc. Chem. Res.*, **1982**, *15*, 275.
- 21 - (a) J.-M. Savéant, *J. Am. Chem. Soc.*, **1987**, *109*, 6788; (b) J.-M. Savéant, *J. Am. Chem. Soc.*, **1992**, *114*, 10595.
- 22 - (a) P. Suppan, *J. Chem. Soc. Faraday Trans.*, **1986**, *82*, 509; (b) E. Vauthey, P. Suppan, and E. Haselbach, *Helv. Chim. Acta.*, **1986**, *69*, 430. Suppan proposed that any screening between the two point charges results only from the polarizability of the solute molecules such that the Coulomb term is no longer solvent dependent, in which case, a modified Coulomb term is applicable where  $n$  is the refractive index and  $r_{DA}$  is the combined effective radius of donor and acceptor:  $-q^2/2n^2r_{DA}$ . We tested the term using the radii of ASC and DTBP determined from their density,  $\rho$ , using the equation  $r_{AB}(\text{Å})=10^8[(3M/4\pi N\rho)^{1/3}]$ , where  $M$  is the molar mass,  $N$  is Avogadro's number and converted it to an effective radius.<sup>9,10</sup> The calculated radii of ASC and DTBP are 2.7 and 2.8 Å, respectively. A *van-der Waals'* radius of 1.9 Å was used for the donors, which is half the thickness of a planar  $\pi$  system providing a centre-to-centre distance between the sensitizer and ASC and DTBP of 4.6 Å and 4.7 Å, respectively. The calculated average contribution from the modified Coulomb term is  $-18 \text{ kcal mol}^{-1}$ , which when applied to the photochemical kinetic data results in an excellent parabolic relationship. This result is likely fortuitous as the validity of a modified Coulomb term has been scrutinised: See M. Tachiya, *Chem. Phys. Lett.*, **1994**, *230*, 491.
- 23 - (a) A. Cardinale, A. A. Isse, A. Gennaro, M. Robert, and J.-M. Savéant, *J. Am. Chem. Soc.*, **2002**, *124*, 13533; (b) C. Costentin, P. Hapiot, M. Médebielle, and J.-M. Savéant, *J. Am. Chem. Soc.*, **2000**, *122*, 5623.
- 24 - A. Houmam and E. M. Hamed, *Phys. Chem. Chem. Phys.* **2012**, *14*, 113.
- 25 - J. F. Callan, A. P. de Silva and N. D. McClenaghan, *Chem. Commun.* **2004**, 2048.
- 26 - Although photoinduced DET is thermodynamically feasible for both ASC and DTBP, other processes may compete, which can result in quantum yields for photoinduced DET less than unity as reported for alkyl halides. See references 3b and 7.
- 27 - L. Ebersson, M. Ekström, T. Lund and H. Lund, *Acta. Chem. Scand.* **1989**, *43*, 101.
- 28 - G. O. Schenck, *Agnew. Chem.*, **1952**, *64*, 12.